Monthly Notices of the ROYAL ASTRONOMICAL SOCIETY

MNRAS **469,** S372–S379 (2017) doi:10.1093/mnras/stx1540
Advance Access publication 2017 June 21

Diamagnetic region(s): structure of the unmagnetized plasma around Comet 67P/CG

P. Henri,[1]★† X. Vallières,[1] R. Hajra,[1] C. Goetz,[2] I. Richter,[2] K.-H. Glassmeier,[2] M. Galand,[3] M. Rubin,[4] A. I. Eriksson,[5] Z. Nemeth,[6] E. Vigren,[5] A. Beth,[3] J.L. Burch,[7] C. Carr,[3] H. Nilsson,[8] B. Tsurutani[9] and G. Wattieaux[10]

[1]*LPC2E, CNRS, F-45071 Orléans, France*
[2]*Institut für Geophysik und extraterrestrische Physik, TU Braunschweig, Mendelssohnstr. 3, D-38106 Braunschweig, Germany*
[3]*Department of Physics, Imperial College London, Prince Consort Road, London SW7 2AZ, UK*
[4]*Physikalisches Institut, University of Bern, Sidlerstrasse 5, CH-3012 Bern, Switzerland*
[5]*Swedish Institute of Space Physics, Ångström Laboratory, Lägerhyddsvägen 1, SE-75120 Uppsala, Sweden*
[6]*Wigner Research Centre for Physics, Budapest, Hungary*
[7]*Southwest Research Institute, PO Drawer 28510, San Antonio, TX 78228-0510, USA*
[8]*Swedish Institute of Space Physics, PO Box 812, SE-981 28 Kiruna, Sweden*
[9]*Jet Propulsion Laboratory, California Institute of Technology, 4800 Oak Grove Drive, Pasadena, CA, USA*
[10]*LAPLACE, Université de Toulouse, CNRS, F-31062 Toulouse, France*

Accepted 2017 June 16. Received 2017 April 3

ABSTRACT

The ESA's comet chaser *Rosetta* has monitored the evolution of the ionized atmosphere of comet 67P/Churyumov–Gerasimenko (67P/CG) and its interaction with the solar wind, during more than 2 yr. Around perihelion, while the cometary outgassing rate was highest, *Rosetta* crossed hundreds of unmagnetized regions, but did not seem to have crossed a large-scale diamagnetic cavity as anticipated. Using *in situ Rosetta* observations, we characterize the structure of the unmagnetized plasma found around comet 67P/CG. Plasma density measurements from RPC-MIP are analysed in the unmagnetized regions identified with RPC-MAG. The plasma observations are discussed in the context of the cometary escaping neutral atmosphere, observed by ROSINA/COPS. The plasma density in the different diamagnetic regions crossed by *Rosetta* ranges from ∼100 to ∼1500 cm^{-3}. They exhibit a remarkably systematic behaviour that essentially depends on the comet activity and the cometary ionosphere expansion. An effective total ionization frequency is obtained from *in situ* observations during the high outgassing activity phase of comet 67P/CG. Although several diamagnetic regions have been crossed over a large range of distances to the comet nucleus (from 50 to 400 km) and to the Sun (1.25–2.4 au), *in situ* observations give strong evidence for a single diamagnetic region, located close to the electron exobase. Moreover, the observations are consistent with an unstable contact surface that can locally extend up to about 10 times the electron exobase.

Key words: plasmas – methods: data analysis – Comets: individual: 67P.

1 INTRODUCTION

Comets are unmagnetized (Auster et al. 2015) Solar system bodies that build up an induced magnetosphere through the interaction of their expanding ionosphere with the incoming solar wind (Cravens & Gombosi 2004). Therefore, besides any locally generated field by currents, the interplanetary magnetic field, frozen into the solar wind plasma (Alfvèn 1957), is the only source of magnetic field at the comet. Close to the cometary nucleus, the plasma becomes collisionally coupled to the radially expanding neutral atmosphere. This prevents the magnetized solar wind from penetrating into the inner cometary regions, which results in the formation of a region void of any significant magnetic field: a diamagnetic cavity (Cravens 1987; Ip & Axford 1987). The fluxgate magnetometer onboard the *Giotto* spacecraft first detected evidence of a diamagnetic cavity at the comet 1P/Halley in 1986, when *Giotto* flew by the comet at a closest distance of 500 km (Neubauer et al. 1986). The spacecraft crossed the cavity surface on its inbound leg at 4470 km and exited the cavity at 4155 km on its outbound leg.

★ E-mail: pierre.henri@cnrs-orleans.fr
† Present address: LPC2E, CNRS, 3A avenue de la Recherche Scientifique, F-45071 Orléans, France.

The ESA's *Rosetta* spacecraft arrived at the target comet 67P/Churyumov–Gerasimenko (hereafter 67P/CG) on 2014 August 6 and detected the first diamagnetic region at the comet on 2015 July 26 with the fluxgate magnetometer of the *Rosetta* Plasma Consortium, RPC-MAG (Goetz et al. 2016b). The diamagnetic region was detected at a cometocentric distance of about 170 km. This is much larger compared to the distances predicted for the diamagnetic cavity from the recent modelling studies (e.g. Koenders et al. 2015; Rubin et al. 2015; Huang et al. 2016), though it may, in part, be associated with the fact that the production rate of the comet was previously underpredicted (Hansen et al. 2016).

No large-scale diamagnetic region, as found around Halley, was reported at 67P/CG. Instead, Goetz et al. (2016a) reported a total of 665 diamagnetic regions detected from 2015 April to 2016 February around 67P/CG, when the heliocentric distance of the comet from the sun varied from 1.8 to 2.4 au. The diamagnetic region(s) were classified into two groups, single events and clustered events, both of which seemed to be distributed randomly. It was statistically shown that the properties of the diamagnetic region(s) depend on the long-term trend of the outgassing rate and that their distribution is organized by theoretical cavity size predicted by neutral drag (Nemeth et al. 2016). Energetic electrons inside the diamagnetic region(s) crossed by *Rosetta*, measured by Ion Electron Sensor (RPC-IES), show a drop in the electron flux for energies above 40 eV (Nemeth et al. 2016; Madanian et al. 2017). These observations indicate a cooling of the electrons in these diamagnetic region(s) through collisions with cometary neutral (Eriksson et al. 2017).

The aim of this work is to explore the structure and dynamics of the unmagnetized thermal plasma around comet 67P/CG. The above-mentioned studies mainly reported the magnetic characteristics and the properties of the energetic electrons during the intervals of diamagnetic region(s) crossings. Nevertheless, the properties of the thermal plasma environment in the diamagnetic region(s) surrounding comet 67P/CG have, as yet, not been well explored. We therefore focus on observations of the cold, unmagnetized plasma that fills the diamagnetic cavity(ies) crossed by *Rosetta*, with the aim to characterize its global structure and stability.

First, we show that the plasma density in the diamagnetic region is entirely determined by the ionization of the cometary neutral atmosphere. In this respect, we obtain an effective total ionization rate from *in situ* measurements. Secondly, although the diamagnetic regions crossed by *Rosetta* seem to be *a priori* almost randomly distributed, we give evidence for a single unmagnetized plasma structure. Thirdly, we show that the most probable location of the boundary between the magnetized and unmagnetized cometary plasmas (contact surface) is located close to the electron exobase, which defines the limit of the electron collisionality. This boundary, between a collisional unmagnetized region and a collisionless (for electron–neutral collisions) magnetized region, has been crossed several times by *Rosetta*. We show that the plasma observations are consistent with an unstable contact surface.

The paper is organized as follows. The *in situ Rosetta* observations of the thermal plasma in the unmagnetized regions encountered by *Rosetta* are described in Section 2 and used to characterize the global structure of the unmagnetized plasma in Section 3. The results are discussed in Section 4.

2 *ROSETTA IN SITU* OBSERVATIONS OF THE UNMAGNETIZED PLASMA DENSITY

To characterize the structure of the unmagnetized plasma observed around comet 67P/CG, we analyse *in situ* data from the *Rosetta*

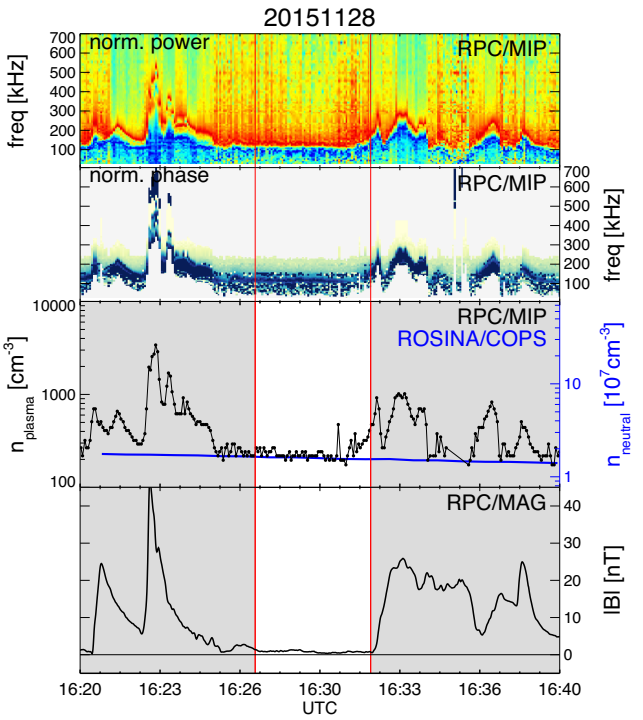

Figure 1. Plasma observations of an isolated diamagnetic region on 2015 November 28. From top to bottom: RPC-MIP mutual impedance spectrogram in amplitude normalized for each spectrum (red: maximum amplitude; blue: minimum amplitude; first panel) and phase (second panel), RPC-MIP plasma density and ROSINA/COPS neutral density (third panel, black and blue lines, respectively) and RPC-MAG magnetic field amplitude (bottom panel). The unmagnetized region is highlighted in white.

Plasma Consortium RPC (Carr et al. 2007) onboard the *Rosetta* orbiter spacecraft (Glassmeier et al. 2007a).

Unmagnetized regions are identified by the RPC-MAG fluxgate MAGnetometers (Glassmeier et al. 2007b). In particular, we make use of the diamagnetic cavity crossings reported in Goetz et al. (2016a). Inside those regions, the plasma density is provided by the Mutual Impedance Probe RPC-MIP (Trotignon et al. 2007). RPC-MIP measures the electric coupling between two antennas, an emitter and a receiver, immersed in a plasma, in a frequency range that contains the plasma frequency. The identification of the plasma frequency from the mutual impedance spectra enables to retrieve the plasma density (Chasseriaux, Debrie & Renard 1972; Storey 1998). The time resolution of MIP mutual impedance spectra measurements, and therefore of derived plasma densities, varies between 2.5 s and 32 s depending on the operational mode used. *In situ* neutral gas density measurements by the Comet Pressure Sensor (COPS) from the *Rosetta* Orbiter Spectrometer for Ion and Neutral Analysis (ROSINA) (Balsiger et al. 2007) are also used for comparison with plasma density measurements. The time resolution of ROSINA/COPS neutral density is 1 min, corresponding to a 10 s average every minute.

Two kinds of diamagnetic regions have been crossed by *Rosetta*: isolated diamagnetic regions and clusters of diamagnetic region(s).

Observations of plasma density variation when crossing an isolated diamagnetic region. An example of diamagnetic region crossed by *Rosetta* on 2015 November 28 is shown in Fig. 1. The unmagnetized region, identified by the RPC-MAG magnetic field data around 16:30 (bottom panel, delimited by two vertical red lines),

is surrounded by magnetized regions (grey parts). The amplitude and phase of the RPC-MIP mutual impedance spectrograms (first and second panels, respectively) show the time variation of the plasma frequency line. The plasma frequency varies between 100 and 600 kHz during this time interval and is observed at about 150 kHz in the unmagnetized region. The plasma density, derived from the identification of the plasma frequency, is shown in the third panel (black points). The unmagnetized plasma density is about 200 cm^{-3} in this example. For comparison, the ROSINA/COPS neutral density is overplotted (same panel, blue points, with another corresponding scale on the right part). The neutral density is constant, about 10^7 cm^{-3}, during the whole time interval. Note that the ionization ratio is low, of the order of $n_{plasma}/n_{neutral} \simeq 10^{-5}$ in this example. This is characteristic of the low-ionization ratio observed during *Rosetta* operations (Galand et al. 2016; Vigren et al. 2016), as the spacecraft remained relatively close to the comet nucleus (about 100 km in this example, from 10 to 1500 km over the mission) compared to the typical ionization length scale $L_i = V_n/\nu_{ion} \simeq 10^7$ km. Here, we have used $V_n \sim 1$ km s^{-1} as the typical cometary neutral escape velocity and $\nu_{ion} \sim 10^{-7}$ Hz as the typical H_2O ionization frequency (Heritier et al. 2017).

In general, the unmagnetized plasma density is observed to be rather steady on the time-scale of the diamagnetic region crossing. On the contrary, the magnetized plasma is characterized by much more dynamics with the formation of large amplitude compressible structures (with relative plasma density variations $\delta n/n > 1$). They are associated with the large magnetic amplitude structures observed at the edges of the diamagnetic regions previously reported in Goetz et al. (2016a). The nature of these magnetized structures is out of the scope of this paper and will be addressed in future works. We concentrate here on the plasma contained in the unmagnetized regions.

Observations of the plasma density profile when crossing clusters of diamagnetic regions. On top of isolated unmagnetized regions, such as the one shown in Fig. 1, *Rosetta* has also often crossed successions of diamagnetic regions, such as illustrated in Fig. 2. The cometary plasma properties are similar to those observed in isolated diamagnetic regions: an almost constant plasma density in the unmagnetized regions, surrounded by high-density variations in the magnetized regions. Note that the magnetized plasma density is of the order of the unmagnetized plasma density or can even be a few times larger in this example. In some other examples (not shown here), the magnetized plasma density has been observed to be slightly smaller than the unmagnetized plasma density, but still of the same order of magnitude. A major property of the plasma observed inside the diamagnetic regions is that its density remains almost constant from one crossing to another. The unmagnetized plasma density actually follows the neutral density variations (third panel: blue dots), typically on time-scales of hours.

Note however that about 15 per cent of the unmagnetized regions crossed by *Rosetta* are characterized by the presence of localized, smooth density variations (not shown here). These unmagnetized compressible structures have amplitudes much smaller than the sharp density variations seen in the adjacent magnetized regions. Their origin is not yet understood and will be studied in future works.

Since the plasma density is observed to be almost constant inside each diamagnetic region crossed by *Rosetta*, we can define a plasma density for each diamagnetic region crossing. When density variations are seen in the unmagnetized regions, we define the plasma density associated with the diamagnetic region crossing as the unmagnetized plasma density before/after these local variations.

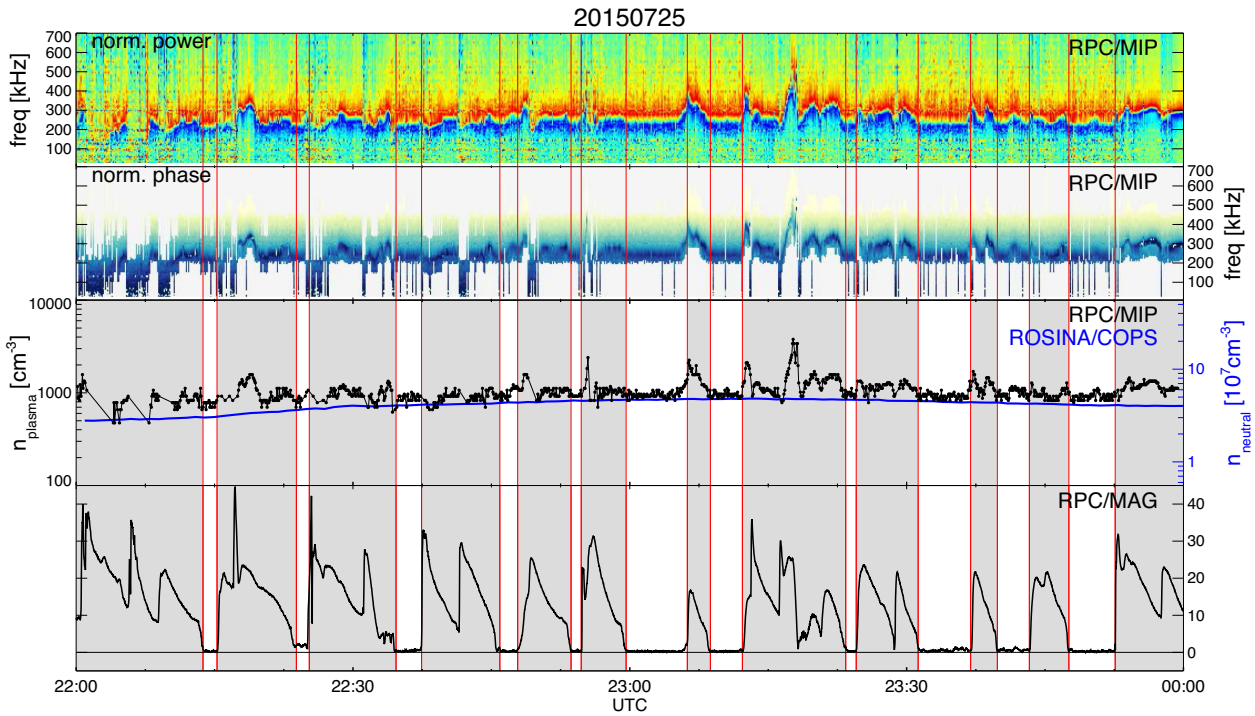

Figure 2. Plasma observations of a succession of diamagnetic region(s) crossings on 2015 July 25. Same panels as Fig. 1.

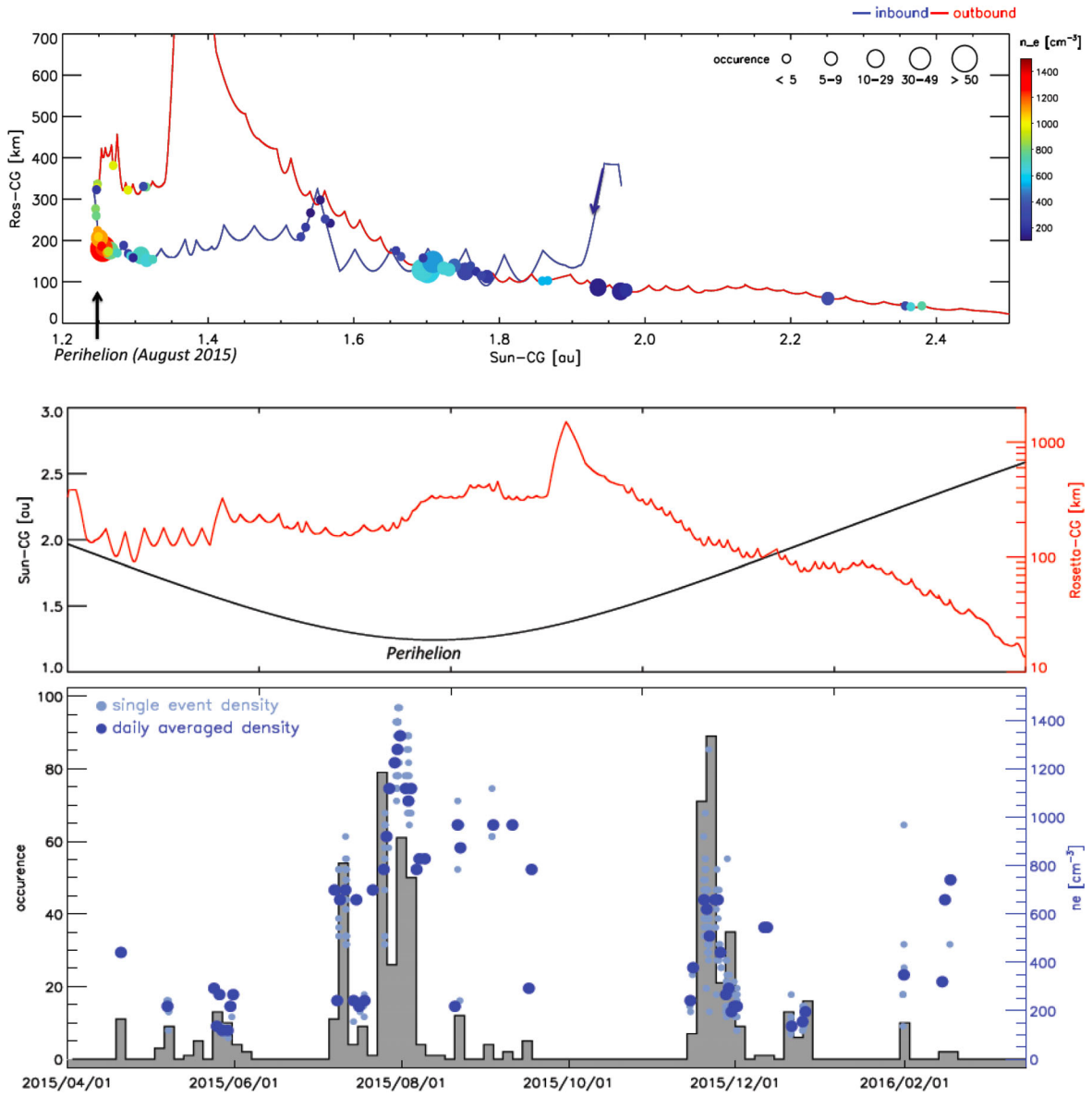

Figure 3. Summary of the different unmagnetized plasma density observations during the *Rosetta* mission, obtained between 2015 April and 2016 February. Top panel: daily average of the unmagnetized plasma density (colour coded) together with the daily number of diamagnetic cavity(ies) crossings at different distances from the Sun and the comet nucleus. Central panel: time evolution of the heliocentric distance of comet 67P/CG (black line) and the cometocentric distance of *Rosetta* (red line) over the same time interval. Bottom panel: time evolution of instantaneous (small blue dots) and daily average (large blue dots) of the unmagnetized plasma density during diamagnetic cavity crossings together with daily occurrence of diamagnetic cavity crossings. The same horizontal scale applies for both central and bottom panels.

Summary of unmagnetized plasma regions crossed during the Rosetta mission. A summary of the plasma density inside the cometary diamagnetic regions encountered by *Rosetta* is shown in Fig. 3. In terms of the heliocentric distance and the cometocentric distance (top panel), the number of diamagnetic regions encountered by *Rosetta* and their associated plasma density both increase (i) as the comet gets closer to the Sun, and therefore as the cometary activity increases, and (ii) as *Rosetta* gets closer to the comet nucleus. Over the entire mission, such diamagnetic regions have been crossed from 2015 April to 2016 February (bottom panel). They have been observed mostly around perihelion, at 1.24 au, reached in 2015 August, and more sporadically as far as heliocentric distances up to about 2.4 au (Goetz et al. 2016a). The corresponding unmagnetized plasma densities, although fairly constant on time-scales of minutes to hours as shown previously in Figs 1 and 2, were observed to vary from ∼100 to ∼1500 cm^{-3} during the whole mission. The higher densities are observed in 2015 July, close to perihelion. Most of the series of diamagnetic region(s) crossings, similar to the one shown in Fig. 2, are observed in the end of July, early August and the end of 2015 November (high crossing occurrence in the bottom panel), which corresponds to local maxima in the observed unmagnetized plasma densities. Note that *Rosetta* has crossed fewer diamagnetic regions during 2015 September–October. Indeed, *Rosetta* moved away from the comet nucleus during this period of highest cometary activity, at cometocentric distances exceeding 300 km, to prevent navigation safety issues. On top of that, a planned excursion brought the *Rosetta* spacecraft up to 1500 km from the comet nucleus in 2015 October.

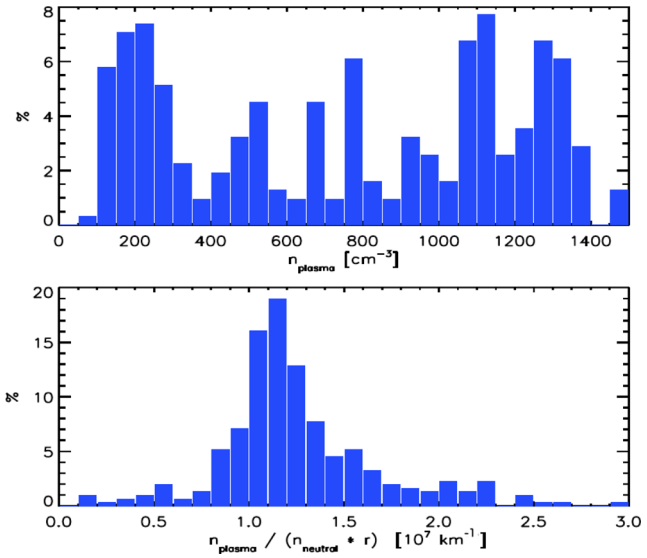

Figure 4. Histograms of the unmagnetized plasma density (top panel) and of $n_{\rm plasma}/(n_{\rm neutral}\dot{c}r)$, representing the plasma-to-neutral density ratio taken into account spherical expansion at the cometocentric distance r (bottom panel).

3 GLOBAL STRUCTURE OF THE UNMAGNETIZED COMETARY PLASMA

As the cometary activity varies significantly during the observations reported in this paper, it is convenient to take it into account through observations of the neutral expanding cometary atmosphere, to better characterize the global structure of the unmagnetized cometary plasma observed close to comet 67P/CG. We show in this section that once the behaviour of the expanding cometary neutral coma has been taken into account (i) we obtain the total effective ionization frequency and (ii) we identify the more likely location of the contact surface, the frontier between the diamagnetic regions and the magnetized cometary plasma.

3.1 Total effective ionization frequency

The plasma density inside the different diamagnetic regions ranges from 100 to 1500 cm^{-3} and shows no particular typical value, as illustrated in the unmagnetized plasma density histogram in the top panel of Fig. 4. This can be understood by the fact that *Rosetta* has witnessed a large range of cometary outgassing activity, at different distances from the nucleus. Once that is taken into account, the unmagnetized plasma density $n_{\rm plasma}$ shows a very predictable behaviour in terms of the neutral density $n_{\rm neutral}$:

$$n_{\rm plasma} \simeq (1.2 \pm 0.3) \times 10^{-7}\, n_{\rm neutral}\, r[\rm km],$$

where cometocentric densities are expressed in the same units (bottom panel) and the cometocentric distance r is expressed in km.

At distances far enough from the nucleus surface, and in the absence of magnetic field (thus in the absence of plasma cross-field acceleration), the cometary plasma density is expected to scale as (Galand et al. 2016; Vigren et al. 2016):

$$n_{\rm plasma} = \nu_{\rm tot}\, r\, n_{\rm neutral}/u_{\rm neutral}.$$

We can therefore constrain the total, average, effective ionization frequency of the expanding cometary coma witnessed by *Rosetta* to

$$\nu_{\rm tot}\,(\rm Hz) \simeq (1.2 \pm 0.3) \times 10^{-7}\, u_{\rm neutral}\,(\rm km\ s^{-1})$$

depending on the actual expanding neutral velocity $u_{\rm neutral}$. Here, we have assumed that the neutral and ion velocities are equal. This is both (i) consistent with the ion composition observed around perihelion (Heritier et al. 2017) and (ii) justified by the absence of cross-magnetic field plasma acceleration, as the $v\times B$ convective electric field vanishes in the unmagnetized region.

The cometary neutral radial velocity has been observed in the range of 0.5–0.8 km s^{-1} by the MIRO instrument in the less active phase of the comet and shown to be positively correlated with outgassing intensity (Gulkis et al. 2015; Lee et al. 2015). Later, near perihelion, the cometary neutral radial velocity was observed by MIRO to be in the range of 0.7 to 1 km s^{-1} (Heritier et al. 2017; Marshall et al. 2017). In addition, still near perihelion, the photoionization frequency of water (the dominant neutral species during this period) is of the order of 3×10^{-7} s^{-1}, while the *local* electron impact ionization frequency, derived from the IES suprathermal electron spectra, is estimated to be of the order of 10^{-8} s^{-1} (Heritier et al. 2017). This yields an expected $\nu_{\rm ph}/u_{\rm neutral} \simeq 3 \times 10^{-7}$ km^{-1}, which is higher than the value derived from the observations (1.2 ± 0.3) 10^{-7} km^{-1}.

The ionization frequency derived from the observations is therefore somewhat lower than the photoionization frequency from solar EUV spectra measured by TIMED/SEE and extrapolated in distance to 67P (Vigren et al. 2015). While there is significant attenuation of the solar radiation in the coma by the gas below a few tens of km, Heritier et al. (2017) have shown that it does not affect significantly the electron density at the location of Rosetta, decreasing it by 5 per cent at 200 km. Dust may however attenuate the incoming solar radiation. Furthermore, the difference found between observed and modelled ionisation frequency may be indicative of some plasma neutralization through dissociative recombination. Indeed this process is neglected in the derivation of the modelled ionisation frequency. However, Heritier et al. (2017) have shown that it can affect significantly the electron density, decreasing it by about 50 per cent at 200 km. Alternatively, it may be a sign of a plasma drift velocity somewhat exceeding the neutral outflow velocity. Indeed, in a model combining the effects of acceleration and collisions, Vigren & Eriksson (2017) have shown that the weak ambipolar electric field set up by the radial gradient in electron pressure can result in the ion-flow speed increasing up to several times the neutral gas expansion velocity, which may explain the lower plasma density observed.

3.2 Plasma–gas collisions

On the one hand, the newborn cometary ions are typically cold with a temperature expected to be of the order of the neutral gas temperature (few 100 K, corresponding to few tenths of meV); on the other hand, the newborn electrons are expected to have a much higher temperature, in the range of 3–10 eV, as observed by RPC-LAP during most of the mission. On top of this warm electron population, signatures of a cold population have been observed around perihelion, in particular inside the diamagnetic regions, with temperatures below 1000 K (0.1 eV) (Eriksson et al. 2017). This cold electron population is understood to have cooled down, through collisions on cometary molecules, which is consistent with the depletion of suprathermal electrons observed during diamagnetic region crossings (Nemeth et al. 2016).

In the inner coma, the thermalization of the weakly ionized cometary plasma is provided by electron–neutral and ion–neutral collisions. In a weekly ionized plasma as encountered by *Rosetta* ($n_{\rm plasma}/n_{\rm neutral} \simeq 10^{-5}$ in the examples shown in Figs 1 and 2),

the electron mean free path $\lambda_{\rm mfp} = 1/n_{\rm neutral}\sigma_{\rm en}$ only depends on the neutral density and the electron–neutral cross-section $\sigma_{\rm en}$. It can be estimated between the comet nucleus and the spacecraft from *in situ* measurements of the neutral density $n_{\rm cops}$ measured by ROSINA/COPS at the spacecraft position $r_{\rm sc}$. The neutral density at a cometocentric distance r falls off as $n_{\rm n}(r) = n_{\rm cops}(r_{\rm sc}/r)^2$ (Bieler et al. 2015; Hässig et al. 2015) so that the electron mean free path varies with the cometocentric distance as $\lambda_{\rm mfp}(r) = (r/r_{\rm sc})^2/(n_{\rm cops}.\sigma_{\rm en})$. We use here an electron–neutral cross-section for 5 eV electron on water molecules $\sigma_{\rm en} \simeq 5 \times 10^{-16}$ cm^2 (Itikawa & Mason 2005).

The location of the electron exobase $L_{\rm e-n}$, the distance to the comet at which the scalelength is equal to the electron mean free path, can therefore be estimated from *in situ* neutral density measurements as $L_{e-n} = n_{\rm cops} r_{\rm sc}^2 \sigma_{\rm en}$. As the plasma density varies in $1/r$, the scalelength is taken here as the plasma density scaleheight that is $n_{\rm plasma}/|\vec{\nabla} n_{\rm plasma}| \approx r$. The electron exobase defines the frontier between a collision-dominated region surrounding the comet, inside which the locally ionized electrons suffer at least one collision with a cometary neutral, and a collisionless region far enough from the comet, where locally ionized electrons are not coupled to the expanding cometary coma and do not cool down (Mandt et al. 2016). The location of the electron exobase is directly associated with the cometary neutral production rate Q and also reads $L_{\rm e-n} = Q\sigma_{\rm en}/4\pi u_{\rm neutral}$.

Fig. 5 shows the daily averaged plasma density observed in the unmagnetized regions crossed by *Rosetta* together with its cometocentric distance (left), the histogram of the plasma densities inside each diamagnetic region (middle) and the histogram of the number of diamagnetic region as a function of the cometocentric distance (right). The top panels essentially contain the same information as Fig. 3. As *Rosetta* covered more cometocentric distances in the range 100–200 km, these distributions are biased towards these distances. All in all, we observe there is no obvious typical location for the position of the boundary between the magnetized and unmagnetized cometary plasmas.

The top panels are actually shown here for a direct comparison with the bottom panels, where the cometocentric distance r is now expressed in terms of the electron exobase $R^\star = r/L_{\rm e-n}$. The different unmagnetized plasma densities, measured at different distances from the comet and for different cometary activity levels, collapse into a single unmagnetized plasma density relation that can be rewritten as

$$n_{\rm plasma} = \frac{\nu_{\rm tot}}{\sigma_{\rm en}\, u_{\rm neutral}} \frac{L_{\rm e-n}}{r} \simeq 2000 \text{ cm}^{-3}/R^*,$$

shown as a red line in the bottom middle panel of Fig. 5. Note that the same radial variation of the cometary plasma density was observed at low cometary activity (at heliocentric distances above 3 au) up to cometocentric distances of 250 km (Edberg et al. 2015), when the plasma could still be considered collisionless but the acceleration of the newborn ions between the comet nucleus and the *Rosetta* was negligible.

When expressed in terms of the electron–neutral collisional distance, which has varied much during the *Rosetta* mission, the data reveal that most of the diamagnetic region crossings have occurred close to the electron exobase (bottom left panel in Fig. 5). This essentially reflects the fact that the various clustered observations of unmagnetized regions, such as the one shown in Fig. 2, have been observed at this distance. Furthermore, the diamagnetic regions crossed at distances much larger than the electron exobase are essentially isolated unmagnetized regions.

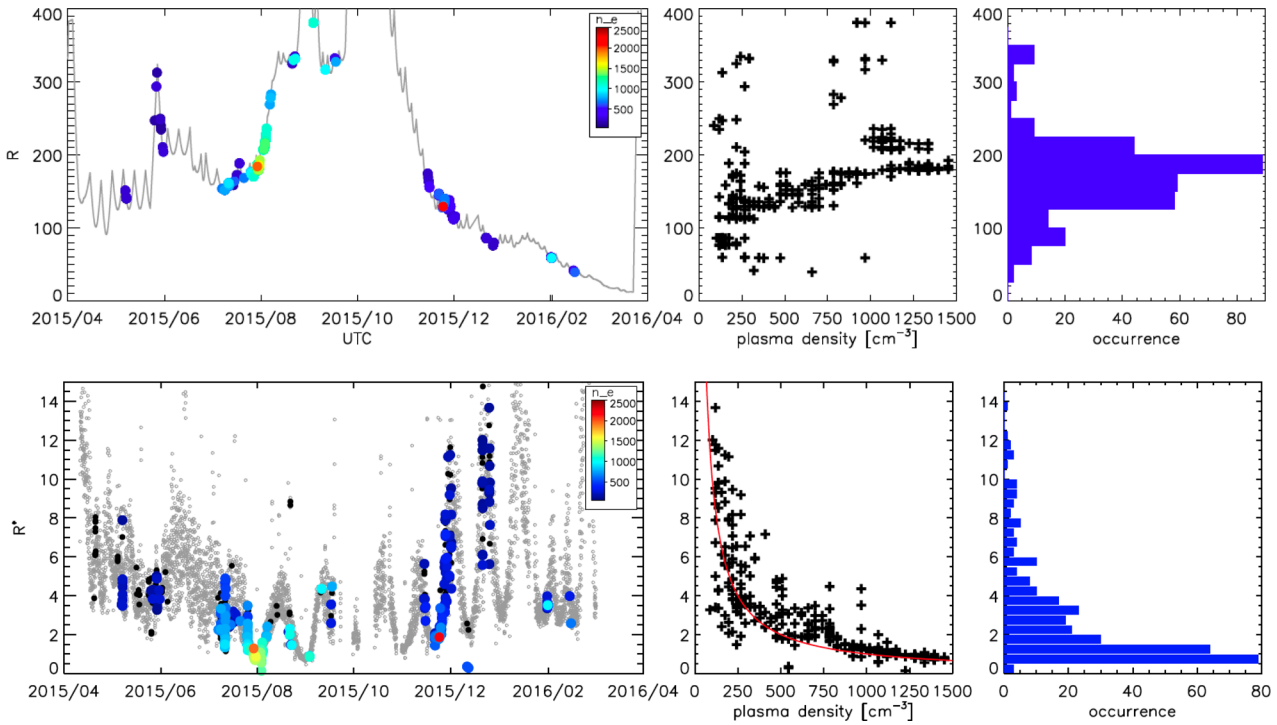

Figure 5. Left-hand panels: *in situ* RPC-MIP plasma density inside the different diamagnetic region(s) crossed by *Rosetta* during the whole mission, shown at the S/C cometocentric distance $r = r_{\rm sc}$ (left-hand panel). Densities are colour coded from 100 to 2500 cm^{-3}. Black dots refer to diamagnetic region crossings during times when no MIP density is available. Grey dots show the 1 d average position to keep track of the evolution of the spacecraft cometocentric distance. Middle panels: variation of the unmagnetized plasma density with the cometocentric distance. Right-hand panels: histogram of the number of diamagnetic cavity crossings with the cometocentric distance. In the top panels the cometocentric distance r is expressed in km, while in the bottom panels the cometocentric distance $R^\star = r/L_{\rm e-n}$ is expressed in terms of the electron exobase $L_{\rm e-n}$ estimated along the comet–spacecraft direction.

4 DISCUSSIONS AND CONCLUSIONS

We have reported (i) *Rosetta in situ* observations of clustered diamagnetic regions with identical plasma densities from one diamagnetic region to the other, located close to the electron exobase, and (ii) observations of isolated unmagnetized plasma structures with similar physical properties as the clustered ones (cold unmagnetized plasma with the same density scaling) that can extend as far as 15 times the cometary electron exobase.

These observations suggest that the clustered diamagnetic regions are the same single region inside which *Rosetta* has entered/left several times, and that the typical position of the contact surface of comet 67P/CG may be located at/close to the electron exobase. This means that the origin of the formation of a diamagnetic region is associated with the limit of *electron* collisionality, which makes sense from a Hall MHD point of view.

Indeed, since the nucleus of comet 67P/CG is unmagnetized (Auster et al. 2015), the only source of the magnetic field observed in the cometary-induced magnetosphere is the interplanetary magnetic field. While the magnetic field can be considered to be frozen into the plasma at large scales, it separates from the (solar wind and newborn cometary) ions at length scales between the ion and electron inertial lengths. These are the typical length scales encountered by *Rosetta* in the close environment of comet 67P/CG. The magnetic field can however still be considered as frozen in the electron fluid at such sub-ion scales. This is why the cometary plasma environment can still carry a large-scale magnetic field, even in the absence of the (deflected) solar wind ions, as the interplanetary magnetic field penetrates deeper in the induced cometary magnetosphere, carried by the electron flow (similar to the ion diffusion region in collisionless magnetic reconnection).

However, close enough to the comet nucleus, in the region where the electrons start to suffer collisions with neutrals, i.e. at distances smaller than the electron exobase, the electron–neutral viscous friction dynamically couples the electron fluid to the radially expanding cometary neutral flow. As a result, the electron fluid should also be directed outward in this collisional region and the interplanetary magnetic field can no longer enter deeper inside the close comet environment: the frontier of the magnetized region therefore scales as the frontier of the electron collisional region.

While *Rosetta* has repeatedly been below the ion exobase (not shown here), it has unfortunately not flown much below the electron exobase (Mandt et al. 2016). The ion exobase is located about 4–16 times further away from the comet nucleus than the electron exobase. In other words, *Rosetta* has been inside the ion–neutral collision-dominated region, much more often than inside the electron–neutral collision-dominated region. This may explain why *Rosetta* has never remained inside the global diamagnetic cavity.

Moreover, the fact that *Rosetta* has entered/left several times the same region on time-scales of minutes (with a quasi-periodicity of about 10 min in the case reported in Fig. 2) suggests that the contact surface may be unstable. Previous authors have found that the cometary boundaries may be unstable to Kelvin–Helmholtz and Rayleigh–Taylor instabilities (Ershkovich & Flammer 1988), as well as convective instabilities (Ershkovich & Israelevich 1993). This unstable boundary would extend pretty far, as indicated by observations of isolated, unmagnetized plasma structures as far as 15 times the cometary electron exobase (Fig. 5, bottom middle and left-hand panels).

Our understanding of how the boundary between the unmagnetized and magnetized cometary plasmas may look like is summarized in Fig. 6. An unstable contact surface (black line) is located close to the electron exobase (blue circle, here with a spherical symmetry, however the electron exobase follows the neutral outgassing asymmetry around the comet nucleus) and extends away in the coma. Two examples of *Rosetta* trajectory around comet 67P/CG (green, dotted lines) illustrate the regions where clustered (resp. isolated) unmagnetized regions are observed closed to (resp. further away from) the electron exobase. Interestingly, similar structures are observed in the Earth's ionosphere. Indeed, after local sunset, due to the absence of plasma production by solar photoionization, high plasma density magnetic flux tubes at the bottom side of the equatorial ionospheric F region are thought to change places with lower density flux tubes from below. This situation is analogous to the hydrodynamic Rayleigh–Taylor instability, where a heavy fluid is located over a light fluid. This interchange of magnetic flux tubes creates a large-scale (tens of kilometres) density perturbation locally, which rapidly penetrates through to the topside of the F region due to the action of perturbation electric fields. This is thought to create what is known as equatorial spread F (see Dungey 1956; Ossakow 1981; Sultan 1996).

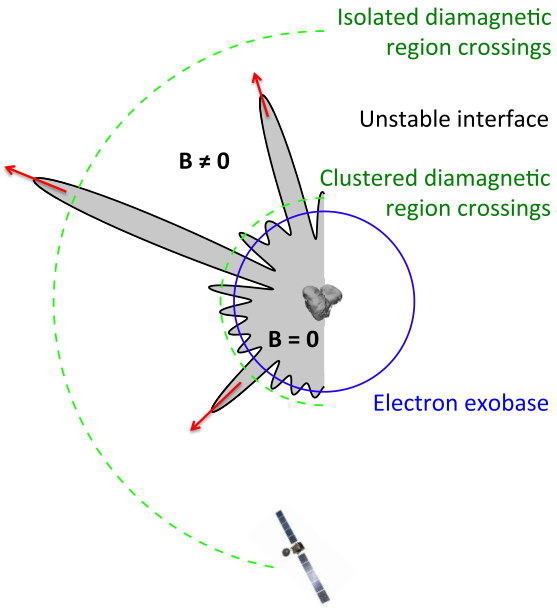

Figure 6. Schematic of unmagnetized versus magnetized plasma observations around comet 67P/CG.

We suggest that the instability observed at the interface between the unmagnetized, collisional and the magnetized, collisionless (for electrons) plasma around comet 67P/CG may be similar to a convective or a Rayleigh–Taylor instability (interchange instability, as called in fusion plasma communities) observed in the Earth's ionosphere. Further works will be required to test deeper this hypothesis.

In this work, we have put the emphasis on the influence of the cometary neutral outgassing, in particular through electron–neutral collisions, on the position of the contact surface. It is worth reminding the influence of the solar wind pressure as well. In particular, changes in the solar wind pressure may also be responsible for the variations observed in the location of the diamagnetic regions. Timar et al. (2017) investigated the influence of the variations of the production rate and the solar wind pressure on the size of a global cavity using the neutral–ion drag model (Cravens 1986) and reported good agreement with the location of diamagnetic regions encountered by *Rosetta*. It is therefore not excluded that a breathing

motion of a global cavity boundary is able to explain some of the observations.

ACKNOWLEDGEMENTS

The *Rosetta* Plasma Consortium (RPC) instrument package consists of five sensors (RPC-ICA, RPC-IES, RPC-LAP, RPC-MAG and RPC-MIP) and a control unit (RPC-PIU). RPC is operated by Imperial College London in cooperation with SwRI, IRFK, IGEP TU Braunschweig, IRFU and LPC2E. The lead funding agencies are CNES, SNSB, NASA, BMWE and DLR, and STFC. The work at LPC2E/CNRS was supported by ESEP, CNES and by ANR under the financial agreement ANR-15-CE31-0009-01. The work on RPC-MAG was financially supported by the German Ministerium fur Wirtschaft und Energie and the Deutsches Zentrum fur Luft- und Raumfahrt under contract 50QP 1401. Work at Imperial College London is supported by STFC of UK under grants ST/K001051/1 and ST/N000692/1. The work of ZN was supported by the János Bolyai Research Scholarship of the Hungarian Academy of Sciences. Portions of this research were carried out at the Jet Propulsion Laboratory, California Institute of Technology under contract with NASA. We acknowledge the staff of CDDP and Imperial College London for the use of AMDA and the RPC Quicklook data base (provided by a collaboration between the Centre de Données de la Physique des Plasmas, supported by CNRS, CNES, Observatoire de Paris and Université Paul Sabatier, Toulouse, and Imperial College London, supported by the UK Science and Technology Facilities Council). The Rosetta data will be made available through ESA's Planetary Science Archive (PSA) Web site.

REFERENCES

Alfvèn H., 1957, Tellus, IX, 92
Auster H.-U. et al., 2015, Science, 349
Balsiger H. et al., 2007, Space Sci. Rev., 128, 745
Bieler A. et al., 2015, A&A, 583, A7
Carr C. et al., 2007, Space Sci. Rev., 128, 629
Chasseriaux J. M. R., Debrie R. D. C., Renard C. R., 1972, J. Plasma Phys., 8, 231
Cravens T. E., 1986, in Battrick B., Rolfe E. J., Reinhard R., eds, ESA SP-250, ESLAB Symposium on the Exploration of Halley's Comet. ESA, Noordwijk, p. 241
Cravens T. E., 1987, Adv. Space Res., 7, 147
Cravens T. E., Gombosi T. I., 2004, Adv. Space Res., 33, 1968
Dungey J., 1956, J. Atmos. Terr. Phys., 9, 304
Edberg N. J. T. et al., 2015, Geophys. Res. Lett., 42, 4263
Eriksson A. I. et al., 2017, A&A, in press
Ershkovich A. I., Flammer K. R., 1988, ApJ, 328, 967
Ershkovich A. I., Israelevich P. L., 1993, ApJ, 411, 891
Galand M. et al., 2016, MNRAS, 462, S331
Glassmeier K.-H., Boehnhardt H., Koschny D., Kührt E., Richter I., 2007a, Space Sci. Rev., 128, 1
Glassmeier K.-H. et al., 2007b, Space Sci. Rev., 128, 649
Goetz C. et al., 2016a, MNRAS, 462, S459
Goetz C. et al., 2016b, A&A, 588, A24
Gulkis S. et al., 2015, Science, 347, aaa0709
Hansen K. C. et al., 2016, MMRAS, 462, S491
Hässig M. et al., 2015, Science, 347, aaa0276
Heritier K. et al., 2017, MNRAS, this issue
Huang Z. et al., 2016, J. Geophys. Res. Space Phys., 121, 4247
Ip W.-H., Axford W. I., 1987, Nature, 325, 418
Itikawa Y., Mason N., 2005, J. Phys. Chem. Ref. Data, 34, 1
Koenders C., Glassmeier K.-H., Richter I., Ranocha H., Motschmann U., 2015, Planet. Space Sci., 105, 101
Lee S. et al., 2015, A&A, 583, A5
Madanian H. et al., 2017, AJ, 153, 30
Mandt K. E. et al., 2016, MNRAS, 462, S9
Marshall D. W. et al., 2017, A&A, 603, A87
Nemeth Z. et al., 2016, MNRAS, 462, S415
Neubauer F. M. et al., 1986, Nature, 321, 352
Ossakow S. L., 1981, J. Atmos. Terr. Phys., 43, 437
Rubin M., Gombosi T. I., Hansen K. C., Ip W.-H., Kartalev M. D., Koenders C., Tòth G., 2015, Earth Moon Planets, 116, 141
Storey L. R. O., 1998, in Pfaff R. F., Borovsky J. E., Young D. T., eds, Mutual-Impedance Techniques for Space Plasma Measurements, in Measurement Techniques in Space Plasma: Fields, Geophys. Monogr. Ser., Vol. 103. American Geophysical Union, Washington DC, p. 155
Sultan P. J., 1996, J. Geophys. Res., 101, 26875
Timar A., Nemeth Z., Szego K., Dosa M., Opitz A., Madanian H., Goetz C., Richter I., 2017, MNRAS, this issue
Trotignon J. G. et al., 2007, Space Sci. Rev., 128, 713
Vigren E., Eriksson A. I., 2017, AJ, 153, 150
Vigren E., Galand M., Eriksson A. I., Edberg N. J. T., Odelstad E., Schwartz S. J., 2015, ApJ, 812, 54
Vigren E. et al., 2016, AJ, 152, 59

This paper has been typeset from a TEX/LATEX file prepared by the author.